European Review for Medical and Pharmacological Sciences 2014; 18: 1723-1734

Role of ubiquitin ligase Cbl-b in B-cell activation of dendritic cells loaded with Tα146-162 in the treatment of experimental autoimmune myasthenia gravis in mice

R. WANG, P. ZHANG, Y. WANG, L. ZHANG

Department of Geriatrics, the Second Xiangya Hospital, Central South University, Changsha, Hunan Province, China

Abstract. – OBJECTIVE: This study aimed to examine the mechanism of Tα146-162-iMDC in the pathogenic intervention of mice with experimental autoimmune myasthenia gravis (EAMG) from the perspective of B-cell activation.

MATERIALS AND METHODS: The mice were divided into three groups, model (A), intervention (B), and control (C), with the intervention of Tα146-162-iMDC. The expressions of Cbl-b mRNA, Syk, Lyn, Btk, and phospholipase C (PLC)-γ2 proteins and their phosphorylated proteins were detected.

RESULTS: The Cbl-b mRNA expression in group A was lower than that in group C ($p < 0.01$) while that in group B increased compared with that in group A ($p < 0.05$), but was lower than that in group C ($p < 0.05$). The expression and phosphorylation of Syk and PLC-γ2 proteins in group A increased compared with those in group C ($p < 0.01$) while those in group B decreased compared with those in group A ($p < 0.05$), but were higher than those in group C ($p < 0.05$). The expression and phosphorylation of Lyn protein in group A decreased compared with those in group C ($p < 0.01$) while those in group B increased compared with those in group A ($p < 0.05$), but were lower than those in group C ($p < 0.05$). The Btk protein expression in group A increased compared with that in group C ($p < 0.01$) while that in group B decreased compared with that in group A ($p < 0.05$), but was still higher than that in group C ($p < 0.05$). However, no difference in phosphorylation levels among the three groups was observed ($p > 0.05$).

CONCLUSIONS: Tα146-162-iMDC intervention can reduce the incidence of EAMG and may be associated with Cbl-b in the negative regulation of B-cell activation.

Key Words:
Experimental autoimmune myasthenia gravis, Tα146-162, Immature myeloid-derived dendritic cells, Cbl-b, B cell.

Introduction

Myasthenia gravis (MG) is typically studied in the model of Experimental Autoimmune Myasthenia Gravis (EAMG), in which 146 to 162 peptides (Tα146-162), an advantage area in T-AChR α subunit, primarily participate in immune response. Immature dendritic cells (DCs) can induce peripheral tolerance. Immature bone marrow dendritic cells (iMDCs) loaded with Tα146-162 (Tα146-162-iMDC) can induce antigen-specific tolerance in T-AchR pre-sensitized T cells[1]. Only a few studies on the influence of B-cell activation have been conducted.

Cbl-b protein with a RING-type ubiquitin-protein ligase enzyme activity can activate the receptor protein tyrosine kinase (PTK) in ubiquitination, which can negatively regulate immune cell receptor signaling, including the down-regulation of TKs and signaling proteins[2-5]. The lack or variation of Cbl-b can cause abnormal immune responses such as autoimmune response, malignant change, and inflammatory reaction[6,7]. Cbl-b inhibits the molecules of T-cell and B-cell activation and adjusts the start threshold of the T-cell receptor (TCR) and B-cell receptor (BCR). Cbl-b regulation in the T-cell and B-cell signaling pathways may be the key to inducing and/or maintaining peripheral immune tolerance and autoimmunity.

B-cell activation is necessary in the pathogenesis of MG/EAMG. BCR constituted by membrane-bound immunoglobulin and Igα/β heterodimers is one of the B-cell surface marker molecules that have key roles in B-cell production, selection, and activation. In BCR signaling pathways, the Src family kinase with PTK activity is the most important, including Src and Lyn. They can be activated into the recruitment and

Corresponding Author: Rong Wang, MD; e-mail: rongwangcn@163.com

activation of PTK Syks and Btk to conduct multiple downstream pathways, including the activations of phospholipase C (PLC)-γ2, Ras, and PI3K pathways, as well as to increase intracellular Ca^{2+} mobilization and cause the activation of transcription factors such as nuclear factor-κB (NF-κB) and nuclear factors of activated T cells. These eventually lead to cell proliferation, differentiation, activation or death. Lyn protein is an important negative regulatory factor in the BCR signaling pathway. Lyn level is reduced in most patients with systemic lupus erythematosus, which is related to enhanced ubiquitination. B-cell proliferation response is also closely related to the change in Lyn expression, indicating that a change in Lyn expression level can affect BCR signaling and B-cell activity[8,9]. Syk, a non-Src protein tyrosine kinase, is the down-regulated target protein in the Src family kinase, which can be used as the upstream pathway factor of Lyn in immature B cells. When B cells lack Syk, loss of reaction to BCR stimulation occurs[10]. Btk is the key molecule in regulating cell survival and cell cycle status in BCR activation signals, and BCR-activated Btk-/-B cell cannot activate the NF-κB signaling pathway[11-13]. PLC-γ2 is one of the key downstream effectors in the BCR signaling pathway that can decompose phosphatidylinositol-4, 5-bisphosphate, release inositol-1, 4, 5-triphosphate and 1, 2-diacylglycerol, and cause intracellular Ca^{2+} pool release; PLC-γ2 also has an important function in NF-κB activation[13]. BCR can cross-link the activation of adjacent Syk and Btk, which are necessary for PLC-γ2 activation and phosphorylation.

After BCR stimulation, tyrosine phosphorylation of Cbl-b requires the participation of Lyn and Syk. After IgM antibody stimulation in Cbl-b-/-mice B cell, Syk phosphorylation is delayed[14,15]. After BCR crosslinking, the Igα/Igβ complex undergoes Igα phosphorylation, leading to Syk recruitment in the Igα SH2 area and subsequent phosphorylation. Cbl-b can adjust the Syk/Ig combo with the combination of Syk Y317 in the tyrosine kinase-binding (TKB) area as well as cause Syk ubiquitination and subsequent denaturation by combining the ubiquitin-conjugating enzyme with the RING area. Cbl-b-/-b cell research indicates that the presence of Igα phosphorylation, not Syk ubiquitination, causes the delayed combination of Igα and phosphorylated Syk; prolonged combination of phosphorylated Syk and Vav; prolonged phosphorylation of B cell linker (BLNK), PLC-γ2, extracellular signal-regulated kinase (ERK), and c-Jun N-terminal kinase (JNK); increased and prolonged Ca^{2+} mobilization; and elevated expression of activation marker CD69[16]. Cbl-b can influence its connection with Igα through Syk degeneration to regulate several Syk downstream signaling pathways, but does not exert any significant effect on Lyn activation. Studies on Cbl-b that lack the DT40 cell indicate that after BCR stimulation, PLC-γ2 activation and Ca^{2+} mobilization occur. Cbl-b has an important function in the Btk-BLNK-PLC-γ2 compound because the latter is necessary in downstream Ca^{2+} mobilization. After BCR crosslinking, prolonged Cbl-b-/-b intracellular Ca^{2+} mobilization is related to loss of Cbl-b and the phosphorylation of Syk, Btk, and PLC-γ2 complex[16-18]. The positive regulation of Cbl-b-dependent Ca^{2+} mobilization requires the TKB area and the end part of COOH, which are related to PLC-γ2. Cbl-b can positively regulate BCR-induced PLC-γ2/Ca^{2+} signal and promote Btk-mediated PLC-γ2 activation, but has no effect on Btk activity[19]. After BCR crosslinking, Cbl-b-/-b intracellular Ca^{2+} mobilization is prolonged, suggesting that it can be related to the loss of Cbl-b and phosphorylation of the Syk-Btk-PLC-γ2 complex[17,18].

In this research, Tα146-162-iMDC was used to intervene in the pathogenesis of EAMG. The changes in Cbl-b expression in the level of gene transcription as well as the expression and phosphorylation of Lyn, Btk, PLC-γ2, and Syk in the BCR signaling pathway were measured to observe the Cbl-b function in the BCR signal transduction pathway and to explore the mechanism of Tα146-162-iMDC in the intervention of EAMG from the perspective of B-cell activation. These details provide a theoretical and experimental basis for clinical MG antigen-specific therapy.

Materials and Methods

Animal handling and grouping

Up to 34 inbred specific pathogen-free (SPF) level C57BL/6J male mice aged 6 to 8 weeks and weighing 14 g to 20 g were used, along with 15 SPF C57BL/6J male mice aged 4 to 6 weeks and weighting 18 g to 22 g, which were supplied by the Experimental Animal Center of Central South University from Shanghai SLAC Laboratory Animal Co., Ltd. The 34 6- to 8-week-old C57BL/6J mice were divided into three groups using the

random number table in SPSS 13.0. In the model group (Group A), 200 μl T-AChR antigen emulsion (200 μg T-AChR, 100 μl CFA, 100 μl PBS) was continuously and subcutaneously injected to the mice shoulders and post-pedes pad three times at 50 μl for each part on day 0, 30, and 60 to induce the EAMG attack[20]. In the intervention group (Group B), T-AChR antigen emulsion was continuously injected three times to the immune animals on day 0, 30, and 60. On day 3, 33, and 63, iMDCs loaded with Tα146-162 (50 μg/ml) were used as intervention. In the control group (Group C), complete Freund's adjuvant (CFA) + phosphate buffered saline (PBS) subcutaneous injection were administered three times on day 0, 30, and 60. On day 3, 33, and 63, 1 ml PBS was used for subcutaneous injection. According to the Berman[20] score standard, the clinical evaluation of EAMG severity was performed and the incidence was calculated in mice that scored more than 1 point. Fifteen 4- to 6-week-old C57BL/6J mice were used for DC procurement and did not participate in the grouping. This study was carried out in strict accordance with the recommendations in the Guide for the Care and Use of Laboratory Animals of the National Institutes of Health. The animal use protocol has been reviewed and approved by the Institutional Animal Care and Use Committee (IACUC) of the Second Xiangya Hospital, Central South University.

Cell culture

The bone marrow was extracted and induced for DC differentiation[21]. For the phenotype analysis of DCs, the cultured DCs were collected and adjusted to 1×10^6/ml cell suspension with PBS, which were stained with Trypan Blue. The staining viability was greater than 95%. The DCs were placed in a test tube, followed by fluorescent antibodies labeled antibody CD11c, CD40, CD86, and MHC-II. The mixture was incubated at 4ºC for 30 min, washed twice with PBS, detected with a flow cytometry (FACS Calibur, BD Bioscience, San Jose, CA, USA), and analyzed with Cell Quest software. Fluorescence-labeled isotype Ig was used as control.

B-lymphproliferation response

The mice were sacrificed at the termination of the experiment. After erythrocyte removal, the splenic cells were incubated with Thy-1 specific monoclonal antibody, and then B-cells were purified under the complement-mediated cytotoxic action. The obtained cells were > 90% $B220^+$. Lymphproliferation responses were detected using Tα146-162 and TAChR as the stimulating antigens, respectively, with KLH as the unrelated antigen for control. Anti-mouse IgM goat specific $F(ab')_2$ antibody was used for positive control. The antibody was displaced with PBS in the negative control. The cells were inoculated onto a 96-pore plate with 4×10^5 each pore. They were divided into five groups with three pores for each group. Afterwards, 20 μg/ml Tα146-162, 0.5 μg/ml TAChR, 100 μg/ml KLH, 10^6 cells/μg anti-mouse IgM goat specific $F(ab')_2$, and PBS were respectively applied to reach a final volume of 200 μl in each pore. The medium contained 10% fetal bovine serum, 100 U/ml penicillin, 100 μg/ml streptomycin, 2 Mm glutaminate, and 3×10^{-5} M 2-ME. The cells were cultured in 5% CO_2 at 37 °C for 5 d. At 18 h before the end of the culture, ^{3}H-TdR (1 μCi/pore) was incorporated. The cells were transferred onto fiberglass filter paper using a DYQ-II multichannel cell collection instrument. The paper was repeatedly washed to remove free ^{3}H-TdR, dried, and then placed into a scintillation fluid-containing plastic tube. Radioactive fluorescence scintillation was counted (CPM), and the mean count of three pores was calculated.

Real-time fluorescence quantitative polymerase chain reaction (RT-PCR)

The primer sequence of Cbl-b and internal reference β-actin were as follows: Cbl-b Sense: 5′GGGTCTCAGAGGCAATG3′, Anti-sense: 5′TTCCTACCAGC TCCAACA3′, with a product of 585 bp; β-actin Sense: 5′CTGTCCCT GTATGCCTCTG 3′, Anti-sense: 5′GGATGTCAACGTCAC-ACTTC 3′, with a product of 451 bp. The mice were executed on day 90, and the groin, popliteal fossa, axillary lymph nodes, and spleens were taken. Total RNA was extracted to determine the concentration and then stored at –70°C in liquid nitrogen. About 2 μl total RNA, 0.5 μl 1 μg/μl Oligo $(dT)_{18}$, and 0.5 μl 40 μ/μl Rnasin were mixed. Diethylpyrocarbonate (DEPC) water was added for a total volume of 12 μl, and the mixture was added into a 0.2 ml PCR reaction tube at 70°C for 5 min. The solution was stored at an ice quencher for 30 s and then briefly centrifuged. Next, 4 μl 5×RT buffer, 2 μl 10 mm deoxyribonucleotide triphosphate (dNTP) mix, and 0.5 μl 40 μ/μl Rnasin were mixed. DEPC water was added for a total volume of 19 μl. The mixture was gently blended and centrifuged for 5 s, and then reacted at 37°C for 5 min. About 1 μl 200 μ/μl M-Mulv

reverse transcriptase was added into the mixture for a total reaction system of 20 μl, which was incubated in the PCR instrument at 42°C for 1 h, denatured at 70°C for 10 min, and cooled on ice for 10 min. The same procedure was used in the blank control, but with DEPC water instead of RNA sample. Up to 1 μl 10 mm dNTP, 2.5 μl 25 mm $MgCl_2$, 2.5 μl 10×T-Aq buffer with $(NH_4)_2SO_4$, 1 μl 10 μM β-actin upstream primer, 1 μl 10 μM β-actin downstream primer, 1 μl 50 μM target gene upstream primer, 1 μl 50 μM target gene downstream primer, 0.4 μl 5 μ/μl T-Aq enzyme, and 2 μl cDNA were added into the 0.2 ml PCR reaction tube. Deionized double-distilled water was added for a final volume of 25 μl for amplification. The PCR product was sampled in 1.5% agarose, with ethidium bromide staining. After electrophoresis, the gel was placed on the T-Anon GIS-2020 electrophoresis gel image analyzer to measure the optical density of each product. The optical density ratio of target gene to that of β-actin was the relative value of the target gene mRNA. The RT-PCR products were collected.

Fluorescence quantitative PCR amplification. The TaqMan probe used in fluorescence quantitative PCR amplification was 5'-(FAM)ATGCCCX(TAMRA)-CCCCCATGCAATCCTGCG Tp-3'. The amplification system with a total volume of 25 μL contained 2 μL of DNA, 0.5 μL of the upstream primer, 0.5 μL of the downstream primer, 0.5 μL of the probe, 0.5 μL of the reference dye Rox reference Dye II, 12.5 μL of Ex taq enzyme premix, and deionized water. The amplification was performed on an ABI Prism 7300 Real-time Fluorescence Quantitative PCR instrument. The amplification conditions consisted of 95 °C for 30 s and 40 cycles of 95 °C for 5 s and 60 °C for 20s. The PCR products were analyzed according to the melting point curve to exclude the possible interference from primer dimmers. Based on the established standard curve, the accurate initial copy numbers of β-actin and Cbl-b in each test sample were calculated automatically. Means were obtained. The relative mRNA copy number of Cbl-b in a test sample was calculated based on the minimum number of cycles satisfying the threshold value (Ct value). The Ct value of each sample (⊿Ct) was calculated based on the following formula: ⊿Ct = Ct (gene of interest) – Ct (the internal reference). ⊿⊿Ct was calculated based the following formula: ⊿⊿Ct = ⊿Ct (model group/intervention group) – ΔCT (control group). The differential fold of the expression of a target gene was calculated using the $2^{-\Delta\Delta C_T}$ method to obtain the relative mRNA template amount of the gene. $2^{-\varnothing\varnothing C_T} > 1$ indicated upregulated expression of the target gene, whereas the value < 1 indicated downregulated expression of the gene.

Standard curve establishment. About 2 μL of β-actin and 2 μL of Cbl-b were respectively applied for fluorescence quantitative PCR, with deionized water as the blank control. Quantitative standard plasmids were prepared using the conventional T-A vector cloning method. The amplification products of β-actin and Cbl-b were collected and cloned to pMDl8-T vectors. The vectors with an inserted fragment were screened. Plasmid DNA was extracted using a plasmid DNA extraction kit and then quantified using an ultraviolet spectrophotometer. After clone number counting, plasmid DNA was diluted to gradient concentrations by 10 times for standard curve establishment.

Western blot

The mice were executed on day 90, and the groin, popliteal fossa, axillary lymph nodes, and spleens were taken. Proteins were extracted from the cytoplasmic lysate. The protein concentration was determined with bicinchoninic acid assay method, and then saved at –70 °C. About 50 μg protein was denaturized and separated with 10% sodium dodecyl sulfate polyacrylamide gel electrophoresis, and then transferred to a nitrocellulose (NC) membranewith constant wet electrical transfer for 1.5 h to 2 h under 150 mA. Afterward, 3% BSA + 5% skimmed milk powder was used to seal a table concentrator at 37°C for 1 h. Rabbit anti-mouse Btk antibody, rabbit anti-mouse Syk antibody, rabbit anti-mouse Lyn antibody, rabbit anti-mouse Btk antibody, rabbit anti-mouse PLC-γ2 antibody, and HRP-p-Tyr mouse monoclonal antibody were diluted with 3% BSA + 5% skimmed milk powder blocking solution (1:500) on a table concentrator at 4°C overnight. These were, then, washed with tris-buffered saline (TBS) three times at room temperature. The horseradish peroxidase (HRP)-labeled goat anti-rabbit secondary antibody (1:2000) was added and reacted at room temperature for 1 h to 1.5 h, after which it was washed with TBS three times at room temperature. Electrochemiluminescence (ECL) liquid was uniformly added on the membrane and stained for 5 min until the ECL fluid dried. The ECL fluid was exposed, developed, and fixed in the darkroom. Adding the secondary antibody on the NC membrane was no longer required as HRP-p-Tyr mouse monoclonal antibody was already added, which could be di-

Table I. DC phenotypes in different phases.

DC	CD11C	CD40	CD86	MHC-II
pDC		—	—	
iMDC	++	+	+	+
mMDC	++	++	++	++

rectly stained. GIS gel image processing system V3.74 was used for film analysis, with GAPDH (1:2000) as the internal reference protein. The experimental methods and procedures were the same as those in the target protein. The ratio of the optical density of target gene to the optical density of GAPDH is the relative value of the target gene.

Co-immunoprecipitation

For Syk, Btk, and PLC-γ2, 5×10^7cells were dissolved in Tris or MES containing 1% NP-40, sodium orthovanadate, and protease inhibitors at each time point. For Cbl-b and Lyn, 2×10^7cells were dissolved in RIPA buffer solution containing 1% NP-40, 0.5% sodium deoxycholate, 0.1% SDS, sodium orthovanadate, and protease inhibitors for cleavage. The lysates were subjected to immunoprecipitation using corresponding specific antibodies. The precipitates were fractioned on SDS-PAGE and then subjected to immunoblotting using phosphotyrosine specific mAb PY20 for tyrosine phosphorylation analysis. Protein expression was also observed.

Statistical analysis

The results were presented as mean ± standard deviation ($\bar{x} \pm s$) and analyzed with SPSS 13.0 software package 8SPSS Inc., Chicago, IL, USA). ANOVA was used in the mean comparison among multiple samples with design group. *T*-test was used in the mean comparison between two samples. Q-test was used in the mean comparison of multiple samples. Mann-Whitney U test was used in the semiquantitative score comparison between the two samples.

Results

Morphological features and phenotypes

After culturing for 24 h, adherent monocytes homogeneously gathered into groups under an inverted phase-contrast microscope. The cells were small and round. The number of cells gradually increased. On day 3, more cells that loosely adhered to the wooden partition could be seen. The cells were small and round and grew in clusters. The volume of the cells gradually increased. On day 6, the phase-contrast microscope showed cells that were irregularly round with adherent growth. A small amount of burr was observed on their surfaces. According to the phenotyping analysis of flow cytometry instruments, $CD11c^+$, $CD40^{low}$, $CD86^{low}$, and $MHC\text{-}II^{low}$ confirmed that the cultured cells were iMDC (Table I, Figures 1).

Mouse behavior and morphology

Different degrees of myasthenia were observed after EAMG pathogenesis of the mice, which manifested as reduced activity, reduced feeding, weak bite, weight loss, arched back, lowered head, vertical tail, and systemic failure. The symptoms of MG could be temporarily improved by neostigmine experiments.

Incidence and clinical scores

The mice in the model group and the intervention group were all out of attack 30 d after the first immunization. On day 39, 2/12 (16.7%) mice were in attack in the model group. On day 57, 1/12 (8.3%) mice were in attack in the intervention group, which was delayed compared with the model group. At the end of the experiment, 9/12 (75%) mice were in attack in the model group and 3/12 (25%) mice in the intervention group, with significant difference in incidence between the two groups ($p < 0.05$). Before the artificial execution, one mouse naturally died due to a serious disease in the model group. No natural death occurred in the intervention group. Since day 66, a significant difference in average clinical scoring was observed between the two groups with 0.75 ± 0.87 vs. 0.17 ± 0.39, respectively ($p < 0.05$). At the end of the experiment, the two groups exhibited 1.67 ± 1.15 vs. 0.33 ± 0.65 clinical scoring, respectively ($p < 0.01$).

B-lymphproliferation response

The cpm value under the stimulation of anti-mouse IgM antibody was noticeably higher than that in any other simulation group, whereas the value under the stimulation of PBS was noticeably lower than that in any other stimulation group. No significant differences were observed among groups A, B, and C. These three groups did not show significant differences in response to KLH, either, with the cpm values close to the PBS group but lower than any other stimulation group. This finding indicates that the cells in

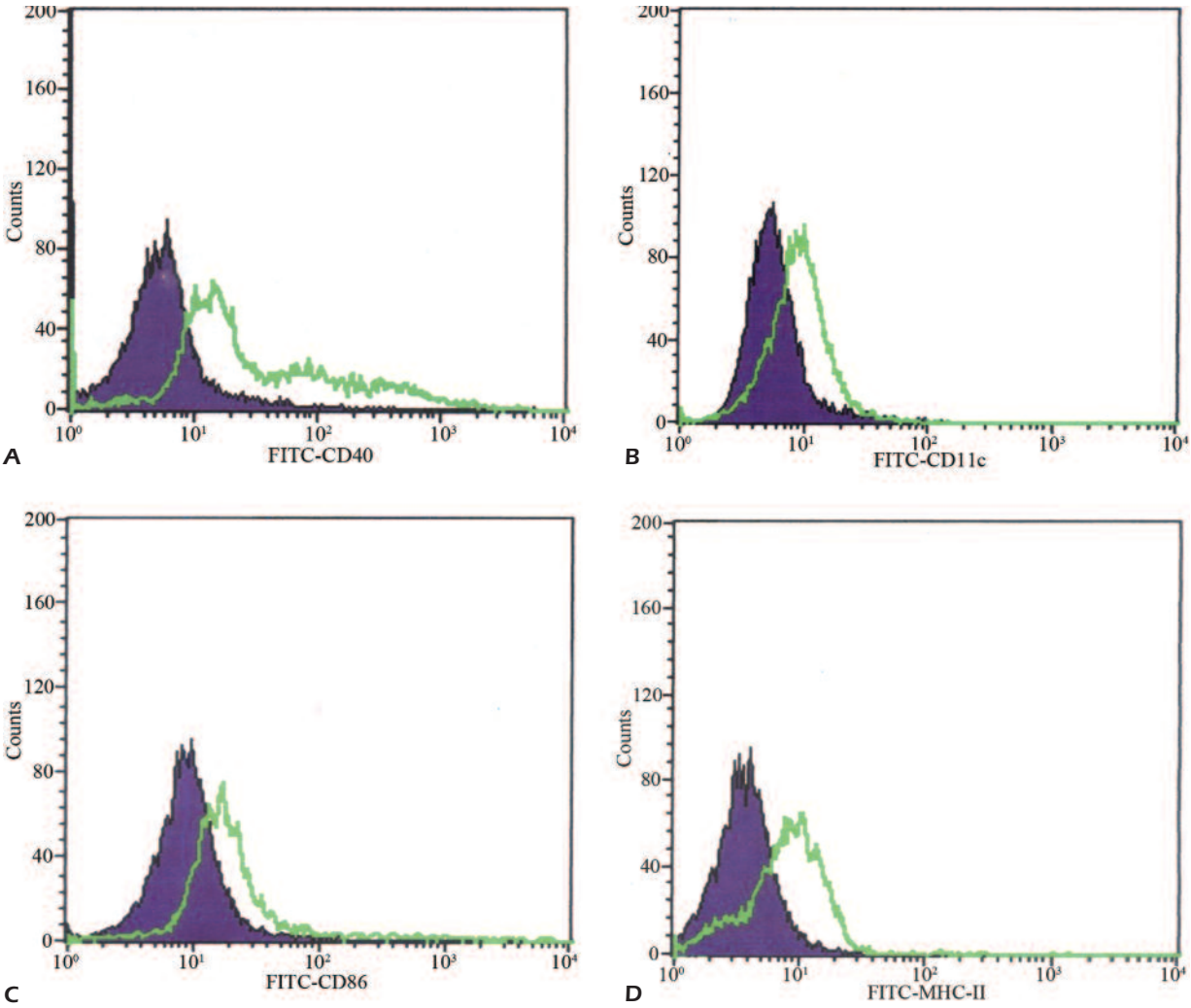

Figure 1. ***A,*** FITC-CD40. ***B,*** FITC-CD11c. ***C,*** FITC-CD86. ***D,*** FITC-MHC-II.

groups A, B, and C did not have proliferative responses to the unrelated antigen. Groups A and B displayed markedly stronger responses to Tα146-162 and TAChR compared with groups C ($p < 0.01$), with those in group A stronger than those in group B ($p < 0.01$). This finding indicates that the cells in both group A and group B had proliferative responses to the specific antigens and that the responses in group B were partially inhibited after intervention. Furthermore, in both groups A and B, the responses to TAChR were slightly more powerful than those to Tα146-162, but without significant differences between the two groups. The results are summarized in Table II.

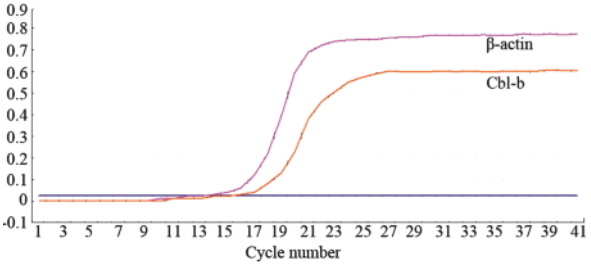

Figure 2. Amplification curves according to RT fluorescence quantitative PCR.

Cbl-b mRNA expression

The RT fluorescence quantitative PCR results showed that the amplification curve of Cbl-b was basically parallel to that of β-actin (Figure 2), which suggests that the amplification efficiencies of Cbl-b and β-actin were fundamentally consistent, and can, therefore, be analyzed using $2^{-\varnothing\varnothing C_T}$. The melting curves showed that both genes were uni-

Table II. B-lymphocyte proliferation (CPM) under the stimulation of different antigens (± s).

Group	Case (n)	External stimulus				
		PBS	T-AChR	Tα146-162	Anti-IgM	KLH
Model	12	903.6 ± 131.2	9423.1 ± 1526.2*§	8203.5 ± 1452.0*§	15047.1 ± 2318.3	1029.5 ± 211.0
Intervention	12	917.4 ± 102.3	3417.5 ± 546.9*	2783.2 ± 525.3*	14059.5 ± 2832.6	987.4 ± 169.8
Control	10	875.2 ± 111.4	1256.3 ± 229.3	1368.4 ± 223.6	13027.3 ± 1866.9	1274.5 ± 215.4

*$p < 0.01$ vs. control group; §$p < 0.01$ vs. intervention group.

Table III. Cbl-b mRNA expression according to RT fluorescence quantitative PCR.

Group	Cases (n)	ΔC_T	$\Delta\Delta C_T$	$2^{-\Delta\Delta C_T}$
Model/spleen	6	3.34 ± 2.69**§	-3.53 ± 2.88**§	0.58 (0.36 - 0.84)
Model/lymph node	6	3.48 ± 3.07**§	-3.46 ± 3.11**§	0.49 (0.35 - 0.72)
Intervention/spleen	6	5.83 ± 3.46*	-1.65 ± 3.16*	0.71 (0.55 - 0.83)
Intervention/lymph node	6	5.69 ± 2.82*	-1.71 ± 2.96*	0.70 (0.46 - 0.88)
Control/spleen	5	7.16 ± 3.01	0.00 ± 0.00	1.00
Control/lymph node	5	7.37 ± 1.27	0.18 ± 0.32	0.98 (0.15 - 1.16)

*$p < 0.05$ vs. control group; **$p < 0.01$ vs. control group; §$p < 0.05$ vs. model group.

modal, and that the melting-out temperature in each curve of the gene was basically consistent, with a sharp peak form and without miscellaneous peaks. These findings suggest that the amplification products in this study had satisfactory specificity. The amplification products were the fragments of interest, and no non-specific products were amplified.

The Cbl-b mRNA expression levels in spleens and lymph nodes in the model group significantly decreased compared with the control group, whereas those in the intervention group increased compared with the model group, but were still lower than those in the control group (Table III, Figure 3).

Expression and phosphorylation of Syk protein

The Syk protein expression levels in spleens and lymph nodes in the model group significantly increased compared with the control group, whereas those in the intervention group decreased compared with the model group, but were still higher than those in the control group. The phosphorylation levels of Syk protein in spleens and lymph nodes in the model group and the intervention group were all higher than those in the control group, whereas those in the intervention group decreased compared with those in the model group, but were higher than those in the control group (Table IV, Figure 4).

Expression and phosphorylation of Lyn protein

The Lyn protein expression levels in spleens and lymph nodes in the model group significantly decreased compared with those in the control group, whereas those in the intervention group significantly increased compared with the model group, but were still lower than those in the con-

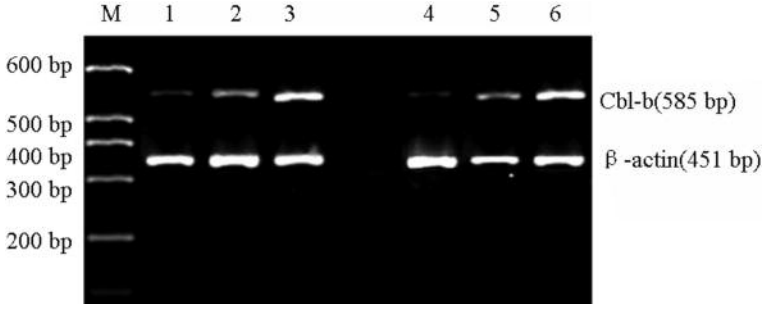

Figure 3. Cbl-b mRNA expression of RT-PCR in each group of mice spleens and lymph nodes. M: marker; 1: Spleens in the model group; 2: Spleens in the intervention group; 3: Spleens in the control group; 4: Lymph nodes in the model group; 5: Lymph nodes in the intervention group; 6: Lymph nodes in the control group.

Table IV. The expression and phosphorylation of Syk protein in spleen and lymph node ($\bar{x} \pm s$).

Groups	n	Protein		Phosphorylation	
		Spleen	Lymph node	Spleen	Lymph node
EAMG	6	$0.822 \pm 0.097^{**\S}$	$0.753 \pm 0.112^{**\S}$	$0.563 \pm 0.062^{**\S}$	$0.469 \pm 0.085^{**\S}$
Treatment	6	$0.662 \pm 0.112^{*}$	$0.527 \pm 0.096^{*}$	$0.421 \pm 0.103^{**}$	$0.369 \pm 0.096^{**}$
Control	5	0.334 ± 0.121	0.365 ± 0.102	0.202 ± 0.087	0.195 ± 0.069

Note: Compared with control group, $^{**}p < 0.01$, $^{*}p < 0.05$; Compared with treatment group, $^{\S}p < 0.05$

Table V. The expression and phosphorylation of Lyn protein in spleen and lymph node ($\bar{x} \pm s$).

Groups	n	Protein		Phosphorylation	
		Spleen	Lymph node	Spleen	Lymph node
EAMG	6	$0.343 \pm 0.100^{**\S}$	$0.244 \pm 0.098^{**\S}$	$0.236 \pm 0.096^{**\S}$	$0.212 \pm 0.097^{**\S}$
Treatment	6	$0.498 \pm 0.097^{*}$	$0.468 \pm 0.078^{*}$	$0.395 \pm 0.104^{*}$	$0.374 \pm 0.077^{*}$
Control	5	0.710 ± 0.183	0.678 ± 0.101	0.596 ± 0.139	0.557 ± 0.098

Note: Compared with control group, $^{**}p < 0.01$, $^{*}p < 0.05$; Compared with treatment group, $^{\S}p < 0.05$

Table VI. The expression and phosphorylation of Btk protein in spleen and lymph node ($\bar{x} \pm s$).

Groups	n	Protein		Phosphorylation	
		Spleen	Lymph node	Spleen	Lymph node
EAMG	6	$0.722 \pm 0.110^{**\S}$	$0.675 \pm 0.101^{**\S}$	0.378 ± 0.097	0.357 ± 0.101
Treatment	6	$0.575 \pm 0.102^{*}$	$0.496 \pm 0.100^{*}$	0.362 ± 0.106	0.316 ± 0.092
Control	5	0.368 ± 0.131	0.334 ± 0.109	0.316 ± 0.125	0.287 ± 0.112

Note: Compared with control group, $^{**}p < 0.01$, $^{*}p < 0.05$; Compared with treatment group, $^{\S}p < 0.05$

trol group. The phosphorylation levels of Lyn protein in spleens and lymph nodes in the model group and the intervention group were all lower than those in the control group, whereas those in the intervention group increased compared with those in the model group, but were lower than those in the control group (Table V, Figure 4).

Expression and phosphorylation of Btk protein

The Btk protein expression levels in spleens and lymph nodes in the model group all increased compared with those in the control group, whereas those in the intervention group decreased compared with those in the model group, but were still higher than those in the control group. No significant difference was observed in Btk protein phosphorylation levels in the spleen and lymph nodes among the three groups (Table VI, Figure 4).

Expression and phosphorylation of PLC-γ2 protein

The PLC-γ2 protein expression levels in spleens and lymph nodes in the model group significantly increased compared with those in the control group, whereas those in the intervention group decreased compared with the model group, but were still higher than those in the control group. The phosphorylation levels of PLC-γ2 protein in spleens and lymph nodes in the model group and the intervention group were all higher than those in the control group, whereas those in the intervention group decreased compared with those in the model group, but higher than those in the control group (Table VII, Figure 4).

Co-immunoprecipitation

Cbl-b phosphorylation was not observed in resting B-cells, but increased immediately after cross linking with BCR. The phosphorylation

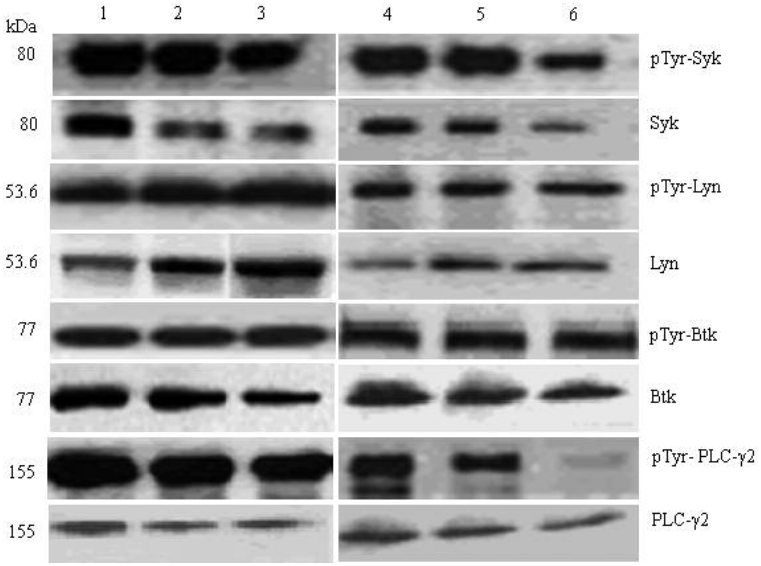

Figure 4. Expression and phosphorylation of Syk, Lyn, Btk, and PLC-γ2 proteins in each group of mice spleens and lymph nodes. 1: Spleens in the model group; 2: Spleens in the intervention group; 3: Spleens in the control group; 4: Lymph nodes in the model group; 5: Lymph nodes in the intervention group; 6: Lymph nodes in the control group.

level started to fall after 5 min of the increase and almost dropped to a nonactivation level after 30 min. The Cbl-b expression in group A significantly decreased compared with that in Group C. Its expression in group B was higher than that in group A but lower than that in group C. These results are shown in Figure 5A. Cbl-b phosphorylation after BCR cross linkage indicates that Cbl-b plays a direct role in the BCR signal pathway.

Syk phosphorylation was not observed in the resting B-cells. After BCR cross linkage, groups A and B exhibited immediately phosphorylation. The phosphorylation levels markedly increased 5 min after cross linkage, and the phosphorylation time prolonged. Group C did not show phosphorylation. The Syk protein expression in Group A significantly increased compared with that in Group C. The protein expression in Group B significantly decreased compared with that in Group A but higher than that in Group C. The phosphorylation levels of Syk protein in both groups A and B were higher than that in group C, with the level in group A higher than that in group B. The results are shown in Figure 5B.

The Lyn phosphorylation levels at all different time points were high in the three groups. After BCR cross linkage, the levels increased slightly, and phosphorylation lasted 30 min. The Lyn protein phosphorylation level in group A noticeably decreased compared with that in Group C. Although the Lyn protein expression level in group B increased compared with that in group A, it was lower than that in group C. The Lyn protein phosphorylation levels in groups A and B were both lower than that in group C. The results are shown in Figure 5C.

Btk phosphorylation was not observed in the resting B-cells in group C. After BCR cross linkage, it increased immediately and reached the peak at 5 min. The Btk protein level in group A increased compared with that in group C. Although the level in group B decreased compared with that in group A, it was higher than that in group C. However, no significant differences in the Btk protein phosphorylation levels were observed among the groups (Figure 5D).

PLC-γ2 phosphorylation was not observed in the resting B-cells in group C. After BCR cross linkage, PLC-γ2 phosphorylation appeared im-

Table VII. The expression and phosphorylation of PLC-γ2 protein in spleen and lymphonode ($\bar{x} \pm s$).

Groups	n	Protein		Phosphorylation	
		Spleen	Lymphonode	Spleen	Lymphonode
EAMG	6	$0.684 \pm 0.144^{**\S}$	$0.655 \pm 0.107^{**\S}$	$0.567 \pm 0.094^{**\S}$	$0.565 \pm 0.105^{**\S}$
Treatment	6	$0.497 \pm 0.102^{*}$	$0.456 \pm 0.093^{*}$	$0.447 \pm 0.110^{*}$	$0.398 \pm 0.109^{*}$
Control	5	0.269 ± 0.131	0.216 ± 0.112	0.219 ± 0.145	0.202 ± 0.119

Note: Compared with control group, $^{**}p < 0.01$, $^{*}p < 0.05$; Compared with treatment group, $^{\S}p < 0.05$

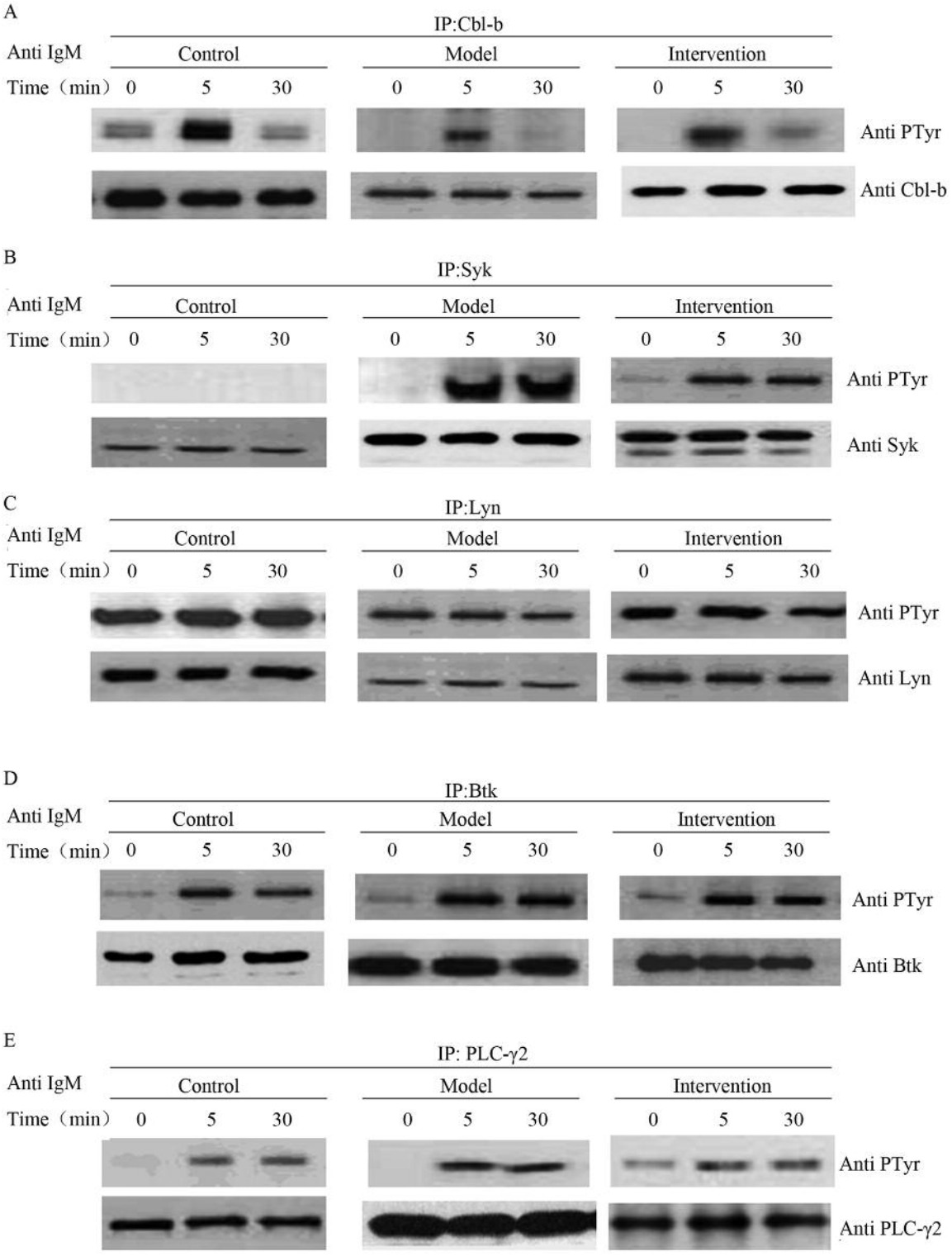

Figure 5. Phosphorylation levels of Cbl-b, Syk, Lyn, Btk, and PLC-γ2 were observed using co-immunoprecipitation.

mediately, reached the peak at 5 min, and started to decrease at 30 min. The PLC-γ2 protein levels in groups A and B significantly increased compared with that in group C, with the level in group B lower than that in group A. The PLC-γ2 protein phosphorylation levels in groups A and B

were higher than that in group C, with the level in group B lower than that in group A. The results are shown in Figure 5E.

Discussion

C57BL/6J mice were subcutaneously injected with *Torpedo californica* AChR (T-AChR) and CFA hybrid emulsion to successfully induce the EAMG model. Tα146-162-iMDC was applied to intervene in the pathogenesis of EAMG. We dynamically observed the expression of ubiquitin ligase Cbl-b in the gene transcription level in EAMG mice and the changes in the expression and phosphorylation of Lyn, Btk, PLc-γ2, and Syk proteins related to BCR-mediated signaling pathways to investigate the function of the Cbl-b to BCR signaling pathway as well as to determine whether Tα146-162- iMDC intervention of EAMG is related to B-cell activation. However, as expected, the results of this study showed that Tα146-162-iMDC can strengthen the negative regulation of Cbl-b in the BCR signaling pathway to restrain auto-reactive B-cell activation and induce B-cell tolerance for inhibition of EAMG attack.

The results of B-lymphproliferation response indicate that the low expression of allostimulatory molecules in Tα146-162 loaded iMDC, such as CD40 and CD86, possibly induces no response or incapability of T-cells, because of the lack of allostimulatory signals during the process of antigen recognition, which is manifested by the proliferative response of antigen specific B lymphocytes weakened and their activation inhibited.

Cbl-b mRNA expression level in the model group decreased compared with that in the control group, but increased compared with that in the model group in mice given Tα146-162-iMDC intervention. This finding indicates that the decreased Cbl-b expression in EAMG mice and the decreased negative regulation of B-cell activation can cause enhanced B-cell activation and pathogenesis in mice. Moreover, Tα146-162-iMDC possibly enhances Cbl-b expression to inhibit B-cell activation. Another research confirmed that Tα146-162-iMDC can induce regulatory T cell (Tr) generation[1]. The two research results indicate that Tα146-162-iMDC can induce the generation of Tr cells to attain high Cbl-b expression, which can restrain the beginning of TCR and BCR and inhibit antigen-specific T-cell and B-cell activation, respectively, thus inducing antigen-specific immune tolerance similar to the research results of previous scholars[2-5]. Lyn protein expression level and phosphorylation level in EAMG mice noticeably decreased compared with those in the control group, indicating that the negative regulation of Lyn decreases in the BCR signaling pathway. Lyn expression level in mice after Tα146-162-iMDC intervention was higher than that in the model group, indicating that Tα146-162-iMDC possibly increases Lyn expression and phosphorylation, and that it may be related to the increase in Cbl-b expression. Syk protein expression level and phosphorylation level in the model mice significantly increased compared with those in the control group, which may be due to the decreased negative regulation of Cbl-b and Lyn in the BCR signaling pathway, the increase in the positive regulation of Syk, the possible increase caused by Tα146-162-iMDC in Cbl-b and Lyn expressions, and the restraint exerted by Lyn phosphorylation on the positive regulation of Syk in the BCR pathway, results similar to those obtained by previous scholars[8-10]. Syk protein expression and increased phosphorylation level in the model group may also be due to the decrease in Cbl-b to reduce Syk ubiquitination and induce Igα phosphorylation; the delayed combination of Igα and phosphorylated Syk; the prolonged combination of phosphorylated Syk and Vav; the prolonged phosphorylation of BLNK, PLC-γ2, ERK, and JNK; the increased and prolonged Ca^{2+} mobilization; and the elevated expression of activation marker CD69[16]. Although the Btk protein expression in EAMG mice was higher than that in the intervention group, no obvious difference was observed among the phosphorylation level model group, the intervention group, and the control group, indicating that the phosphorylation of Btk protein in EAMG mice was unaffected. Thus, Tα146-162-iMDC does not affect the positive regulation of Btk through Cbl-b in the BCR signaling pathway. The expression and phosphorylation of positive regulatory factor PLC-γ2 in the BCR signaling pathway in the model group increased, indicating that after AchR stimulation to BCR, PLC-γ2 is activated for phosphorylation and causes BCR conduction along the downstream signaling pathway to induce B-cell activation. Tα146-162-iMDC decreases mice PLC-γ2 expression and phosphorylation, which are related to increased Cbl-b expression and inhibited PLC-γ2 phosphorylation, consistent with the research results by Daniel[19].

Conclusions

By strengthening the negative regulation of Cbl-b in the BCR signaling pathway, autoreactive B-cell activation is restrained. Induced B-cell tolerance is another possible mechanism in Tα146-162-iMDC intervention of EAMG attack. The study supplemented the previous mechanism of Tα146-162-iMDC intervention of EAMG attack, including T-cell activation and complement, as well as provided new ideas and approaches for MG/EAMG treatment. The mechanism of Tα146-162-iMDC in B-cell activation in the process of EAMG attack was only observed in this study, so no intervention was present in the established EAMG model. The treatment effect of Tα146-162-iMDC is uncertain. Further research should mainly focus on the curative effect of Tα146-162-iMDC on MG/EAMG and other mechanisms.

Conflict of Interest

The Authors declare that there are no conflicts of interest.

References

1) Swaminathan G, Tsygankov AY. The Cbl family proteins: ring leaders in regulation of cell signaling. J Cell Physiol 2006; 209: 21-43.
2) Bionaz M, Periasamy K, Rodriguez-Zas SL, Everts RE, Lewin HA, Hurley WL, Loor JJ. Old and new stories: revelations from functional analysis of the bovine mammary transcriptome during the lactation cycle. PLoS One 2012; 7: e33268.
3) Yamashima T. 'PUFA-GPR40-CREB signaling' hypothesis for the adult primate neurogenesis. Prog Lipid Res 2012; 51: 221-231.
4) Jun JE, Goodnow CC. Scaffolding of antigen receptors for immunogenic versus tolerogenic signaling. Nat Immunol 2003; 4: 1057-1064.
5) Liu YC. Ubiquitin ligases and the immune response. Annu Rev Immunol 2004; 22: 81-127.
6) Yi C, Ma M, Ran L, Zheng J, Tong J, Zhu J, Ma C, Sun Y, Zhang S, Feng W, Zhu L, Le Y, Gong X, Yan X, Hong B, Jiang FJ, Xie Z, Miao D, Deng H, Yu L. Function and molecular mechanism of acetylation in autophagy regulation. Science 2012; 336: 474-477.
7) Shahaf G, Gross AJ, Sternberg-Simon M, Kaplan D, DeFranco AL, Mehr R. Lyn deficiency affects B-cell maturation as well as survival. Eur J Immunol 2012; 42: 511-521.
8) Flores-Borja F, Kabouridis PS, Jury EC, Isenberg DA, Mageed RA. Decreased Lyn expression and translocation to lipid raft signaling domains in B lymphocytes from patients with systemic lupus erythematosus. Arthritis Rheum 2005; 52: 3955-3965.
9) Ying H, Li Z, Yang L, Zhang J. Syk mediates BCR- and CD40-signaling integration during B cell activation. Immunobiology 2011; 216: 566-570.
10) Vargas-Hernández A, López-Herrera G, Maravillas-Montero JL, Vences-Catalán F, Mogica-Martínez D, Rojo-Domínguez A, Espinosa-Rosales FJ, Santos-Argumedo L. Consequences of two naturally occurring missense mutations in the structure and function of Bruton agammaglobulinemia tyrosine kinase. IUBMB Life 2012; 64: 346-353.
11) Wang LD, Lopes J, Cooper AB, Dang-Lawson M, Matsuuchi L, Clark MR. Selection of B lymphocytes in the periphery is determined by the functional capacity of the B cell antigen receptor. Proc Natl Acad Sci U S A 2004; 101: 1027-1032.
12) Halcomb KE, Contreras CM, Hinman RM, Coursey TG, Wright HL, Satterthwaite AB. Btk and phospholipase C gamma 2 can function independently during B cell development. Eur J Immunol 2007; 37: 1033-1042.
13) Sohn HW, Gu H, Pierce SK. Cbl-b negatively regulates B cell antigen receptor signaling in mature B cells through ubiquitination of the tyrosine kinase Syk. J Exp Med 2003; 197: 1511-1524.
14) Katkere B, Rosa S, Drake JR. The Syk-binding ubiquitin ligase c-Cbl mediates signaling-dependent B cell receptor ubiquitination and B cell receptor-mediated antigen processing and presentation. J Biol Chem 2012; 287: 16636-16644.
15) Tüzün E, Saini SS, Morgan BP, Christadoss P. Complement regulator CD59 deficiency fails to augment susceptibility to actively induced experimental autoimmune myasthenia gravis. J Neuroimmunol 2006; 181: 29-33.
16) Kitaura Y, Jang IK, Wang Y, Han YC, Inazu T, Cadera EJ, Schlissel M, Hardy RR, Gu H. Control of the B cell-intrinsic tolerance programs by ubiquitin ligases Cbl and Cbl-b. Immunity 2007; 26: 567-578.
17) Depoil D, Weber M, Treanor B, Fleire SJ, Carrasco YR, Harwood NE, Batista FD. Early events of B cell activation by antigen. Sci Signal 2009; 2: pt1.
18) Daniel JL, Dangelmaier CA, Mada S, Buitrago L, Jin J, Langdon WY, Tsygankov AY, Kunapuli SP, Sanjay A. Cbl-b is a novel physiologic regulator of glycoprotein VI-dependent platelet activation. Biol Chem 2010; 285: 17282-17291.
19) Yang H, Tüzün E, Alagappan D, Yu X, Scott BG, Ischenko A, Christadoss P. IL-1 receptor antagonist-mediated therapeutic effect in murine myasthenia gravis is associated with suppressed serum proinflammatory cytokines, C3, and anti-acetylcholine receptor IgG1. J Immunol 2005; 175: 2018-2025.
20) Berman PW, Patrick J. Experimental myasthenia gravis: a murine system. J Exp Med 1980; 151: 204-223.
21) Horwitz DA, Zheng SG, Gray JD, Wang JH, Ohtsuka K, Yamagiwa S. Regulatory T cells generated ex vivo as an approach for the therapy of autoimmune disease. Semin Immunol 2004; 16: 135-143.